

DEUTSCHES ELEKTRONEN-SYNCHROTRON DESY

DESY SR-82-12

August 1982

Eigentum der
Property of **DESY** Bibliothek
library

Zugang: 17. Jan. 2002
Accessions:

Keine Ausleihe
Not for loan

CALCULATED PHOTOEMISSION SPECTRA OF THE 4f STATES IN THE RARE EARTH METALS

by

F. Gerken

II. Institut für Experimentalphysik, Universität Hamburg

NOTKESTRASSE 85 · 2 HAMBURG 52

DESY behält sich alle Rechte für den Fall der Schutzrechtserteilung und für die wirtschaftliche
Verwertung der in diesem Bericht enthaltenen Informationen vor.

DESY reserves all rights for commercial use of information included in this report, especially in
case of filing application for or grant of patents.

To be sure that your preprints are promptly included in the
HIGH ENERGY PHYSICS INDEX ,
send them to the following address (if possible by air mail) :

DESY
Bibliothek
Notkestrasse 85
2 Hamburg 52
Germany

CALCULATED PHOTOEMISSION SPECTRA OF THE 4f STATES IN THE RARE
EARTH METALS

F. Gerken

II. Institut für Experimentalphysik, Universität Hamburg,
D-2000 Hamburg 50, FRG

Recent high quality X-ray photoemission experiments on rare earth metals (Lang et al. 1981) have proved quite successfully the validity of the fractional parentage scheme for calculating the relative photoemission intensities of the different atomic 4f final state multiplets (Cox 1975, Cox et al. 1981). Differences between theory and experiment especially for the heavy rare earths were explained as an indication of the breakdown of LS-coupling (Russell-Saunders coupling) in which the calculation was carried out for most of the elements while intermediate coupling was used only in some restricted energy ranges.

An improvement of the theory becomes desirable since surface sensitive photoemission experiments in the VUV region show different binding energies for bulk and surface core levels in the rare earth metals (Kammerer et al. 1982, Gerken 1982, Gerken et al. 1982a, Gerken et al.) ("surface shift"). The spectra consist of a superposition of multiplet lines originating from bulk atoms and from the surface atoms which are rigidly shifted to higher binding energies by about 0.5 to 0.7 eV. Bulk and surface components can only be disentangled by use of an accurate theory for the photoemission intensities (Kammerer et al. 1982, Gerken et al. 1982a).

Therefore a complete calculation in intermediate coupling was carried out. The result is tabulated and the multiplet lines convoluted with Doniach Sunčić lineshapes (Doniach and Sunčić 1970) are presented as calculated spectra which compare well with experimental results on rare earth metals.

The calculation of the energy levels in intermediate coupling was already carried out by Carnall et al. and the energy positions of the multiplet lines were tabulated up to about 50000 cm^{-1} for all the rare earth ions. This energy corresponds to the highest structure which could be identified in their absorption spectra of rare earth ions in dilute acid solution.

Since in photoemission, however, a 4f multiplet splitting up to about 12 eV ($\sim 100000 \text{ cm}^{-1}$) appears in the spectra and the eigenfunctions of the levels are required for the photoemission intensity calculation, the energy level calculation was repeated. A detailed treatment of the theory has been discussed by Wybourne and Sobelman (Wybourne 1965, Sobelman 1979). Therefore only the general outline of the calculation needs to be included here.

According to the theory of Racah (Racah 1949) the different states of the f-shell may be classified in LS-coupling notation by the quantum numbers W, U, v, S, L, J, M_J . The quantum numbers S, L, J, M_J represent, as usual, the total spin and orbital angular momentum, the resultant total angular momentum and its projection. The seniority number v and the quantum numbers U and W are necessary to distinguish between states with the same S, L, J, M_J assignment which appear in the f-shell. W and U consist of three and two integer numbers respectively,

$$W = (w_1 w_2 w_3), \quad U = (u_1 u_2) \quad (1)$$

The energy level structure of the f^N configurations arises mainly from electrostatic and spin orbit interaction between the f electrons. The electrostatic part of the total energy matrix can be written in the form (Racah 1949)

$$E_C = \sum_{k=0}^3 e_k E^k \quad (2)$$

The e_k 's represent the angular part while the E^k are linear combinations of the Slater Radial Integrals F_k . This representation was chosen by Racah since it has simple transformation properties with respect to the symmetry groups used to classify the states. The electrostatic interaction is diagonal in the quantum numbers S and L and independent of

J and M_J but it is not diagonal in the additional quantum numbers W, U and v . Therefore the e_k 's are generally matrices which have been calculated and tabulated completely (Nielson and Koster 1964). The electrostatic electron-electron interaction is responsible for a breakdown of the degeneration of different LS-terms in a f^N configuration.

The energy of the spin orbit interaction E_{SO} is given by

$$E_{SO} = \xi_{4f} \cdot \sum_{i=1}^N (\vec{s}_i \cdot \vec{\ell}_i) = \xi_{4f} \cdot A_{SO} \quad (3)$$

ξ_{4f} represents the radial integral and A_{SO} is the angular part of the spin orbit interaction. s and ℓ are the spin and orbital angular momentum of the electrons. The matrix elements of E_{SO} can be calculated by the formula (Wybourne 1965)

$$(\ell^N \tau_{SLJM_J} | \xi_{nl} \sum_{i=1}^N (\vec{s}_i \cdot \vec{\ell}_i) | \ell^N \tau' S'L' JM_J) = \xi_{nl} \cdot (-1)^{J+L+S'} \cdot \begin{Bmatrix} L & L' & 1 \\ S & S & J \end{Bmatrix} \cdot [\ell(\ell+1)(2\ell+1)]^{1/2} \cdot (\ell^N \tau_{SL} || V^{11} || \ell^N \tau' S'L') \quad (4)$$

τ represents the additional quantum numbers W, U and v .

The reduced matrix elements V^{11} are given by

$$(\ell^N \tau_{SL} || V^{11} || \ell^N \tau' S'L') = N \cdot [s(s+1)(2s+1)(2S+1)(2L+1)(2S'+1)(2L'+1)]^{1/2} \cdot \sum_{\tau'' S'' L''} G_{\tau'' S'' L''}^{\tau SL} \cdot G_{\tau'' S'' L''}^{\tau' S'L'} \cdot (-1)^{S''+L''+S+L+s+\ell} \cdot \begin{Bmatrix} S & S' & 1 \\ s & s & S'' \end{Bmatrix} \cdot \begin{Bmatrix} L & L' & 1 \\ \ell & \ell & L'' \end{Bmatrix} \quad (5)$$

$G_{\tau'' S'' L''}^{\tau SL}$ are the fractional parentage coefficients (fpc) which give the construction of a state $(\ell^N \tau_{SL})$ from the possible states $(\ell^{N-1} \tau'' S'' L'')$. They have been calculated by Koster and Nielson for p, d and f electrons

using the methods given by Racah. The spin orbit interaction is diagonal in the quantum number J , independent of M_J but not diagonal in the other quantum numbers. If the spin orbit interaction parameter ξ_{NL} exceeds a certain value, the off-diagonal matrix elements cannot be neglected and the diagonalization of the total energy matrix results in a mixing of different LS states with the same total angular momentum J (intermediate coupling).

In the theory given above the important influence of configuration interaction has not been considered. This interaction can be treated in a second order perturbation theory. For f^N configurations it may be written as (see e.g. Carnall et al. 1968, Wybourne 1965 and References therein)

$$E_{CI} = \alpha \cdot L \cdot (L+1) + \beta \cdot G(G_2) + \gamma \cdot G(R_7) \quad (6)$$

α, β and γ are linear combinations of radial integrals, $G(G_2)$ and $G(R_7)$ are eigenvalues of Casimir's operator of the groups G_2 and R_7 , respectively, and may be calculated using the quantum numbers U and W (Racah 1949, Judd 1959)

$$G(G_2) = g(U) = g(u_1 u_2) = (u_1^2 + u_1 u_2 + u_2^2 + 5u_1 + 4u_2)/12 \quad (7)$$

$$G(R_7) = g(W) = g(w_1 w_2 w_3) = (w_1(w_1+5) + w_2(w_2+3) + w_3(w_3+1))/10 \quad (8)$$

For the energy level calculation the total energy matrices including all interactions described above were built up for all possible quantum numbers J using the radial energy parameters published by Carnall et al. They are comprised in Table I. The parameter E^0 in equation (2) was omitted since it only has the effect of shifting the center of gravity of the entire f^N configuration without contributing to the structure of the configuration. The matrices were diagonalized for all states from the

configuration $4f^2$ up to $4f^{13}$ except for $4f^7$ where only the three highest multiplicities (8, 6 and 4) were considered. This restriction is only due to the fact that about 35% of more than 20000 fpc's that exist for the states from f^2 to f^7 belong to the states of f^7 with the lowest multiplicity 2. Since only small changes in the eigenfunctions are expected for the two highest multiplicities which show up in the photoemission spectrum of Tb ($4f^8 \rightarrow 4f^7$) when the multiplicity 2 is neglected, the time for the laborious task of putting these fpc's into the computer was spared.

The resultant eigenfunctions and eigenvalues of the calculation fill about 100 pages which is rather too lengthy to be published here. The energy levels are characterized by the remaining good quantum numbers J and M_J . The eigenfunctions give the composition of this intermediate coupling states in LS-basis and may be written in the form

$$|4f^N JM_J\rangle = \sum_{\tau SL} C_{\tau SL}^J |4f^N \tau SL JM_J\rangle \quad (9)$$

$$\text{with } \sum_{\tau SL} |C_{\tau SL}^J|^2 = 1 \quad (10)$$

The calculation of the photoemission intensities in the sudden approximation has been discussed in detail by Cox (Cox 1975) for the LS-coupling case. In a recent paper (Cox et al. 1981) this theory is extended to Bremsstrahlung Isochromat Spectroscopy (BIS) which may be viewed as an inverse photoemission process. For BIS the intensity calculation is also derived for the more general intermediate coupling case. This can easily be transformed to the photoemission case. According to this theory the intensity for a transition from the initial state $|z^N JM_J\rangle$ to the final state $|z^{N-1} J' M_J'\rangle$ is proportional to

$$N \cdot (2J'+1) \cdot \sum_j \left\{ (2j+1) \left[\sum_{\tau' S' L'} C_{\tau' S' L'}^J \cdot C_{\tau' S' L'}^{J'} \cdot [(2S+1)(2L+1)]^{1/2} \right] \right. \\ \left. \cdot \begin{Bmatrix} s & \ell & j \\ s & L & J \\ s' & L' & J' \end{Bmatrix} \cdot G_{\tau' S' L'}^{\tau S L} \right\}^2 \quad (11)$$

j is the total angular momentum of a single electron which is $5/2$ and $7/2$ for f electrons with $\ell=3$. The sum of the intensities of a state ℓ^N equals the number of electrons N . Formulas for the $9-j$ and $6-j$ symbols which appear in equation (4), (5) and (11) were taken from the appendix of a text book from Messiah (Messiah 1979).

The calculation is performed for all $4f^N \rightarrow 4f^{N-1}$ transitions except for the trivial cases $4f^2 \rightarrow 4f^1$ (Pr) and $4f^{14} \rightarrow 4f^{13}$ (Yb,Lu) where only the two final states $^2F_{5/2}$ and $^2F_{7/2}$ appear.

The lowest energy level for each $4f^N$ configuration represents its ground state and the pertinent eigenfunctions were therefore used as initial state in the intensity calculation. The results are given in Table 2. The different final states are characterized by the main LS-contribution of the eigenfunction.

In addition, the multiplet lines are convoluted with Doniach-Sunjic lineshapes (Doniach and Sunjic 1970) and Gaussian profiles to account for the many-body reaction on the sudden creation of a core hole in a metal and for an experimental resolution, respectively, and plotted on a binding energy scale (Fig. 1). The parameters are tabulated in Table 3. They are close to the values used by Lang et al. to fit their experimental results. An energy scaling factor of 1.1 is applied in the spectra except for Eu compared to the energy positions tabulated in Table 3 in order to account

for the different nuclear charge in photoemission final states and the absorption experiments from Carnall et al. Finally a background of scattered electrons computed with a program which simulates the travel of the photoelectrons through the metal (Gerken 1982) is added to the curves.

As a result the calculated spectra agree well with the photoemission spectra published by Lang et al. A strong improvement of the intermediate coupling calculation compared to the LS-coupling for the heavy rare earth metals is obtained. Since the calculation presented here includes all possible final states of the different $4f^N$ -configurations, several structures appear at relatively high binding energies. Although these structures have only low intensities they should show up also in experimental spectra and demonstrate the quality of the theory.

Some small differences in the relative intensities of multiplet lines between theory and experiment may be explained by the following arguments:

It has been shown that the binding energy of the multiplets in the rare earth metals is different for bulk and surface atoms (Kammerer et al. 1982, Gerken et al. 1982a). Although the mean free path in XPS is already as large as 20 Ångström it can be estimated (Barth 1982) that a fraction of 10 to 20% surface emission should be contained in angular integrated spectra. Depending on the structure of the spectrum and the value for the surface shift this fact may influence the relative intensity of the multiplet structure or only change the fit-parameters slightly (e.g. the asymmetry parameter).

Furthermore for Er and Tm the $3d \rightarrow 4f$ excitation energy (Fischer and Baun 1967) is close to the photon energy in XPS chosen by Lang et al. Recent photoemission experiments with synchrotron radiation in the energy range of the $4d \rightarrow 4f$ excitation ("resonant photoemission" experiments) demonstrate that intershell interaction gives rise to drastic changes in the relative intensities of the 4f multiplet structures which can not be described in the framework of the fractional parentage theory (Gerken et al. 1982b). Similar effects cannot be excluded also for the $3d \rightarrow 4f$ excitations.

The agreement between the theory presented here and experiments, however, is very satisfactory and stresses the importance of a full intermediate coupling calculation in the rare earth. The present theory may be adapted to other problems by use of the tabulated eigenvalues and intensities. Additional high resolution photoemission experiments with different photon energies (e.g. Mg K α , Cu K α or synchrotron radiation), carried out in the same excellent quality as the results from Lang et al., would be helpful to exclude surface effects and intershell interaction and test the validity of the theory.

References:

- Barth J. 1982 Thesis University of Hamburg.
- Carnall W.T., Fields P.R. and Rajnak K. 1968 J. Chem. Phys. 49 4412-4455.
- Cox P.A. 1975 Structure and Bonding 24 59.
- Cox P.A., Lang J.K. and Baer Y. 1981 J. Phys. F: Met. Phys. 11 113.
- Doniach S. and Sunjic M. 1970 J. Phys. C: Solid State Phys. 3 285.
- Fischer D.W. and Baun W.L. 1967 J. Applied Phys. 38 4830.
- Gerken F. 1982 Thesis University of Hamburg.
- Gerken F., Barth J., Johansson L.I. and Flodström A., to be published.
- Gerken F., Barth J., Kammerer R., Johansson L.I. and Flodström A. 1982a Surface Science 117 468.
- Gerken F., Barth J. and Kunz C. 1982b Contributed paper to the International Conference on X-Ray and Atomic Inner-Shell Physics, to be published in the American Institute of Physics Conference Proceedings series.
- Judd B.R. 1959 Proc. Roy. Soc. A 250 562.
- Kammerer R., Barth J., Gerken F., Johansson L.I. and Flodström A. 1982 Solid St. Commun. 41 427.
- Lang J.K., Baer Y. and Cox P.A. 1981 J. Phys. F: Met. Phys. 11 121.
- Messiah A. 1979 *Quantum mechanics II*, de Gruyter, Berlin, New York.
- Nielson C.W. and Koster G.F. 1964 *Spectroscopic Coefficients for p^n , d^n , and f^n Configurations*, M.I.T. Press, Cambridge, Mass.
- Racah G. 1949 Phys. Rev. 76 1352.
- Sobelman I.I. 1979 *Atomic Spectra and Radiative Transitions*, Springer Verlag, Berlin, Heidelberg, New York.
- Wybourne B.G. 1965 *Spectroscopic Properties of Rare Earths*, John Wiley & Sons, New York.

Figure Captions:

Fig. 1 : Theoretical spectra of the rare earth metals on a binding energy scale relativ to the lowest multiplet. The calculated multiplet lines from Table 2 are convoluted with Doniach Sunjic lineshapes using the parameters comprised in Table 3. A calculated background is added and the resultant curve folded with a Gaussian profil of 0.2 eV FWHM to account for an experimental resolution.

Table 2 : Energy positions and intensities of the multiplet lines for the transitions $f^N \rightarrow f^{N-1}$ with N=3 to N=13. Intensities lower than 0.01 are omitted. For the initial states the complete eigenfunctions and for the final state only the main contribution in the representation $(w_1 w_2 w_3)$, $(u_1 u_2)$, seniority, $2S+1$, L are given.

Table 1

Radial energy parameters which were used to diagonalize the total energy matrices. Energies are given in cm^{-1} . The values are taken from Carnall et al.

f^N	Element	E^1	E^2	E^3	ξ_{4f}	α	β	γ
f^2	Pr^{3+}	4548.2	21.937	466.73	740.75	21.255	-799.94	1342.9
f^3	Nd^{3+}	4739.3	23.999	485.96	884.58	0.5611	-117.15	1321.3
f^4	Pm^{3+}	4921.6	24.522	525.53	1000.8	10.991	-244.88	789.74
f^5	Sm^{3+}	5496.9	25.809	556.40	1157.3	22.250	-742.55	796.64
f^6	Eu^{3+}	5573.0	26.708	557.39	1326.0	25.336	-580.25	1155.7
f^7	Gd^{3+}	5761.0	28.02	582.0	1450.0	22.55	-103.7	997.0
f^8	Tb^{3+}	6021.5	29.03	608.54	1709.5	20.131	-370.21	1255.9
f^9	Dy^{3+}	6119.6	30.012	610.14	1932.0	37.062	-1139.1	2395.3
f^{10}	Ho^{3+}	6440.6	30.22	624.39	2141.3	23.635	-807.2	1278.4
f^{11}	Er^{3+}	6769.9	32.388	646.62	2380.7	18.347	-509.28	649.71
f^{12}	Tm^{3+}	7142.4	33.795	674.27	2628.7	14.677	-631.79	0

Photoemission-Intensity in intermediate couplings
Transition from 4f 3 to 4f 2

Initial state eigenfunction: J = 4.5

0.9846	(111)(20)	3	4	I
0.0564	(210)(11)	3	2	H
-0.1635	(210)(21)	3	2	H

Final state intensities:

	J	E (eV)	Intensity
(110)(10)	2	3 F 2.0	0.6080
(110)(10)	2	3 F 3.0	0.7805
(110)(11)	2	3 H 4.0	0.0000
(110)(11)	2	3 H 5.0	0.2576

Photoemission-Intensity in intermediate couplings
Transition from 4f 5 to 4f 4

Initial state eigenfunction: J = 2.5

0.9788	(110)(11)	5	6	H
-0.1246	(111)(20)	3	4	G
0.0293	(211)(20)	5	4	G
0.0350	(211)(21)	5	4	G
-0.1523	(211)(30)	5	4	G

Final state intensities:

	J	E (eV)	Intensity
(111)(20)	4	5 D 0.0	3.7045
(111)(20)	4	5 D 1.0	3.7654
(111)(10)	4	5 F 1.0	1.5247
(111)(20)	4	5 D 2.0	3.8641
(111)(20)	4	5 G 2.0	2.2017
(111)(10)	4	5 F 2.0	1.5760
(211)(21)	4	3 G 3.0	2.6040
(111)(20)	4	5 G 3.0	2.2510
(111)(10)	4	5 F 3.0	1.6802
(111)(20)	4	5 G 4.0	2.4897
(211)(30)	4	3 H 4.0	2.1359
(111)(20)	4	5 I 4.0	0.0000
(111)(20)	4	5 I 5.0	0.1832
(111)(20)	4	5 I 6.0	0.3827

Photoemission-Intensity in intermediate couplings
Transition from 4f 4 to 4f 3

Initial state eigenfunction: J = 4.0

0.9850	(111)(20)	4	5	I
0.0777	(110)(11)	2	3	H
0.0835	(211)(21)	4	3	H
-0.1270	(211)(30)	4	3	H

Final state intensities:

	J	E (eV)	Intensity
(111)(10)	3	4 F 1.5	1.4130
(111)(20)	3	4 G 2.5	2.1123
(111)(10)	3	4 F 2.5	1.5428
(111)(20)	3	4 G 3.5	2.3213
(210)(20)	3	2 G 3.5	2.0622
(111)(20)	3	4 G 4.5	2.3833
(111)(20)	3	4 I 4.5	0.0000
(111)(20)	3	4 I 5.5	0.2327
(111)(20)	3	4 I 6.5	0.4804

Photoemission-Intensity in intermediate couplings
Transition from 4f 6 to 4f 5

Initial state eigenfunction: J = 0.0

0.9666	(100)(10)	6	7	F
-0.1868	(111)(20)	4	5	D
0.1676	(210)(21)	6	5	D

Final state intensities:

	J	E (eV)	Intensity
(211)(30)	5	4 P 2.5	4.0663
(110)(11)	5	6 P 2.5	3.4330
(110)(11)	5	6 P 2.5	2.9791
(211)(21)	5	4 F 2.5	2.7364
(110)(10)	5	6 F 2.5	0.8813
(110)(11)	5	6 H 2.5	0.0000
(110)(11)	5	6 P 3.5	3.2910
(110)(10)	5	6 F 3.5	0.9863
(110)(11)	5	6 H 3.5	0.1285

Photoemission-Intensity in intermediate couplings
Transition from 4f 9 to 4f 8

Photoemission-Intensity in intermediate couplings
Transition from 4f 8 to 4f 7

Initial state eigenfunction: J = 6.0

0.9786	(100)(10)	6	7	F
-0.1431	(111)(20)	4	5	G
0.0565	(210)(20)	6	5	G
0.1341	(210)(21)	6	5	G
0.0130	(210)(21)	6	5	H

Initial state eigenfunction: J = 7.5

0.9707	(110)(11)	5	6	H
-0.1101	(111)(20)	3	4	I
-0.2109	(211)(30)	5	4	I
-0.0233	(211)(21)	5	4	K

Final state intensities:

Final state intensities:

J	E (eV)	Intensity
(200)(20)	7 6 D 2.5	5.0783
(110)(11)	5 6 F 2.5	4.0627
(110)(10)	5 6 F 3.5	6.7767
(200)(20)	7 6 G 3.5	6.1717
(200)(20)	7 6 D 3.5	5.0511
(110)(11)	5 6 F 3.5	4.0106
(0)(0)	7 8 S 3.5	0.0000
(110)(10)	5 6 F 4.5	6.7887
(200)(20)	7 6 G 4.5	6.1569
(200)(20)	7 6 D 4.5	4.9330
(110)(11)	5 6 H 5.5	7.3015
(211)(21)	5 4 H 5.5	7.1523
(110)(10)	5 6 F 5.5	6.7117
(200)(20)	7 6 G 5.5	6.1621
(200)(20)	7 6 I 5.5	4.5280
(110)(11)	5 6 H 6.5	7.4495
(211)(21)	5 4 H 6.5	7.0398
(200)(20)	7 6 G 6.5	6.3591
(200)(20)	7 6 I 6.5	4.5512
(220)(20)	7 4 I 7.5	8.2659
(220)(21)	7 4 L 7.5	7.3060
(110)(11)	5 6 H 7.5	7.2400
(200)(20)	7 6 I 7.5	4.5523
(200)(20)	7 6 I 8.5	4.5214

J	E (eV)	Intensity
(210)(21)	6 5 F 4.0	4.3759
(210)(21)	6 5 D 4.0	2.5045
(100)(10)	6 7 F 4.0	0.4045
(111)(10)	4 5 F 5.0	8.0699
(210)(21)	6 5 G 5.0	5.2199
(210)(21)	6 5 F 5.0	4.3078
(210)(21)	6 5 G 5.0	3.5028
(100)(10)	6 7 F 5.0	0.2505
(221)(31)	6 3 I 6.0	6.0375
(221)(31)	6 3 H 6.0	5.8580
(210)(20)	6 5 G 6.0	5.0630
(210)(11)	6 5 H 6.0	4.0594
(210)(21)	6 5 G 6.0	3.4414
(100)(10)	6 7 F 6.0	0.0000
(111)(20)	4 5 I 7.0	8.0008
(221)(30)	6 3 I 7.0	7.7136
(221)(31)	6 3 K 7.0	6.3025
(210)(21)	6 5 H 7.0	5.8097
(221)(31)	6 3 K 7.0	5.5909
(210)(21)	6 5 K 7.0	5.1427
(210)(20)	6 5 I 7.0	4.5570
(210)(11)	6 5 H 7.0	3.9107
(210)(21)	6 5 L 7.0	3.6192
(221)(31)	6 3 L 8.0	7.9523
(111)(20)	4 5 I 8.0	7.7813
(210)(21)	6 5 K 8.0	5.0534
(210)(20)	6 5 I 8.0	4.3670
(210)(21)	6 5 L 8.0	3.6057
(210)(21)	6 5 K 9.0	4.8361
(210)(21)	6 5 L 9.0	3.5206
(210)(21)	6 5 L 10.0	3.3584

34301

Table 2b

Photoemission-Intensity in intermediate coupling
Transition from 4f10 to 4f 9

Initial state eigenfunction: J = 8.0

0.9666	(111)(20)	4	5	I
0.1180	(211)(21)	4	3	K
-0.2224	(211)(30)	4	3	K
-0.0318	(211)(21)	4	3	L

Final state intensities:

	J	E (eV)	Intensite
(211)(21)	5	4 F 4.5	2.6050
(110)(10)	5	6 F 4.5	1.1174
(110)(11)	5	6 H 4.5	0.9424
(211)(21)	5	4 G 5.5	6.1565
(211)(20)	5	4 G 5.5	4.3673
(211)(11)	5	4 H 5.5	4.2120
(211)(30)	5	4 G 5.5	2.8184
(110)(10)	5	6 F 5.5	0.9499
(110)(11)	5	6 H 5.5	0.7101
(111)(20)	3	4 I 6.5	9.4050
(221)(31)	5	2 I 6.5	6.7236
(211)(11)	5	4 H 6.5	6.2930
(211)(30)	5	4 H 6.5	5.9177
(211)(20)	5	4 I 6.5	5.3287
(211)(21)	5	4 K 6.5	4.1767
(211)(11)	5	4 H 6.5	4.1649
(211)(30)	5	4 I 6.5	3.2680
(110)(11)	5	6 H 6.5	0.4257
(111)(20)	3	4 I 7.5	9.2255
(211)(30)	5	4 K 7.5	6.8926
(221)(30)	5	2 K 7.5	6.1742
(211)(20)	5	4 I 7.5	5.1511
(211)(21)	5	4 K 7.5	3.9883
(211)(30)	5	4 I 7.5	3.0013
(110)(11)	5	6 H 7.5	0.0000
(221)(21)	5	2 L 8.5	6.9797
(211)(30)	5	4 K 8.5	6.6976
(211)(30)	5	4 M 8.5	3.8207
(211)(21)	5	4 K 8.5	3.2594
(211)(21)	5	4 L 9.5	3.9812
(211)(30)	5	4 M 9.5	3.3653
(211)(30)	5	4 M 10.5	3.2564
			1.3334

Photoemission-Intensity in intermediate coupling
Transition from 4f11 to 4f10

Initial state eigenfunction: J = 7.5

0.9853	(111)(20)	3	4	I
-0.1702	(210)(21)	3	2	K
-0.0173	(210)(21)	3	2	L

Final state intensities:

	J	E (eV)	Intensite
(211)(21)	4	3 F 4.0	4.7644
(111)(20)	4	5 G 4.0	4.3037
(111)(20)	4	5 G 4.0	3.1919
(111)(10)	4	5 F 4.0	2.2975
(211)(30)	4	3 G 5.0	8.5036
(211)(21)	4	3 H 5.0	7.4712
(111)(20)	4	5 G 5.0	3.4185
(111)(20)	4	5 G 5.0	2.9516
(111)(10)	4	5 F 5.0	1.9141
(111)(20)	4	5 I 5.0	1.3742
(110)(11)	2	3 H 6.0	11.5694
(211)(21)	4	3 K 6.0	7.2880
(211)(21)	4	3 H 6.0	6.9850
(211)(11)	4	3 H 6.0	6.5996
(211)(20)	4	3 I 6.0	4.9281
(211)(30)	4	3 H 6.0	3.4212
(111)(20)	4	5 G 6.0	2.7293
(111)(20)	4	5 I 6.0	1.0580
(211)(30)	4	3 I 7.0	8.0653
(211)(21)	4	3 K 7.0	7.2367
(220)(21)	4	1 K 7.0	6.2424
(211)(20)	4	3 I 7.0	4.7595
(211)(21)	4	3 L 7.0	4.7040
(211)(30)	4	3 K 7.0	3.2280
(111)(20)	4	5 I 7.0	0.6243
(211)(21)	4	3 K 8.0	6.8333
(220)(22)	4	1 L 8.0	4.5174
(211)(30)	4	3 K 8.0	2.6318
(111)(20)	4	5 I 8.0	0.0000
(211)(21)	4	3 L 9.0	3.5880
(211)(30)	4	3 M 10.0	4.2380
			1.3609

34300

Table 2c

Photoemission-Intensity in intermediate coupling
Transition from 4f13 to 4f12

Initial state eigenfunction: J = 3.5

Photoemission-Intensity in intermediate coupling
Transition from 4f12 to 4f11

1.0000 (100)(10) 1 2 F

Initial state eigenfunction: J = 6.0

0.9956	(110)(11)	2	3 H
0.0932	(200)(20)	2	1 I

Final state intensities:

	J	E (eV)	Intensity
(210)(21)	3	2 D 2.5	6.0651
(111)(20)	3	4 D 2.5	4.7686
(210)(20)	3	2 D 2.5	4.3010
(111)(20)	3	4 G 2.5	4.1256
(111)(10)	3	4 F 2.5	2.7230
(100)(10)	1	2 F 3.5	12.0490
(210)(21)	3	2 F 3.5	6.8249
(111)(20)	3	4 D 3.5	4.8410
(111)(20)	3	4 G 3.5	4.1555
(111)(20)	3	4 G 3.5	3.3651
(111)(10)	3	4 F 3.5	2.5079
(210)(21)	3	2 G 4.5	8.4283
(210)(11)	3	2 H 4.5	5.9047
(111)(20)	3	4 G 4.5	3.3921
(111)(10)	3	4 F 4.5	2.9689
(111)(10)	3	4 F 4.5	1.8603
(111)(20)	3	4 I 4.5	1.5002
(210)(11)	3	2 H 5.5	6.3090
(210)(20)	3	2 I 5.5	5.0704
(111)(20)	3	4 G 5.5	3.2717
(210)(21)	3	2 H 5.5	2.3740
(111)(20)	3	4 I 5.5	1.2532
(210)(20)	3	2 I 6.5	5.4061
(210)(21)	3	2 K 6.5	4.0880
(111)(20)	3	4 I 6.5	0.8057
(210)(21)	3	2 K 7.5	3.4330
(111)(20)	3	4 I 7.5	0.0000
(210)(21)	3	2 L 8.5	5.1545

Final state intensities:

	J	E (eV)	Intensity
(0)(0)	0	1 S 0.0	9.8428
(110)(11)	2	3 F 0.0	4.3932
(110)(11)	2	3 F 1.0	4.4752
(110)(11)	2	3 F 2.0	4.7101
(200)(20)	2	1 D 2.0	3.4503
(110)(10)	2	3 F 2.0	1.8491
(110)(10)	2	3 F 3.0	1.7739
(200)(20)	2	1 G 4.0	2.6250
(110)(11)	2	3 H 4.0	1.5520
(110)(10)	2	3 F 4.0	0.6955
(110)(11)	2	3 H 5.0	1.0151
(200)(20)	2	1 I 6.0	4.3002
(110)(11)	2	3 H 6.0	0.0000

Photoemission-Intensity in intermediate coupling
Transition from 4f 7 to 4f 6

Initial state eigenfunction: J = 3.5

0.9869	(0)(0)	7	8 S
0.1600	(110)(11)	5	6 P
-0.0117	(200)(20)	7	6 D

Final state intensities:

	J	E (eV)	Intensity
(100)(10)	6	7 F 0.0	0.0000
(100)(10)	6	7 F 1.0	0.0473
(100)(10)	6	7 F 2.0	0.1301
(100)(10)	6	7 F 3.0	0.2368
(100)(10)	6	7 F 4.0	0.3591
(100)(10)	6	7 F 5.0	0.4911
(100)(10)	6	7 F 6.0	0.6287

34299

Table 2d

Table 3

Parameters of the Doniach-Sunjić curves from Fig. 1.

Element	Nd	Pm	Sm	Eu ₂ O ₃	Eu	Gd	Tb	Dy	Ho	Er	Tm	Yb ₂ O ₃
Transition	$f^3 \rightarrow f^2$	$f^4 \rightarrow f^3$	$f^5 \rightarrow f^4$	$f^6 \rightarrow f^5$	$f^7 \rightarrow f^6$	$f^7 \rightarrow f^6$	$f^8 \rightarrow f^7$	$f^9 \rightarrow f^8$	$f^{10} \rightarrow f^9$	$f^{11} \rightarrow f^{10}$	$f^{12} \rightarrow f^{11}$	$f^{13} \rightarrow f^{12}$
HHHM γ (eV)	0.37	0.2	0.16	0.2	0.06	0.18	0.17	0.17	0.12	0.12	0.12	0.2
Asymmetry α	0.12	0.12	0.11	0.2	0.18	0.19	0.16	0.13	0.19	0.16	0.21	0.2
Scaling factor	1.1	1.1	1.1	1.1	1.0	1.1	1.1	1.1	1.1	1.1	1.1	1.1

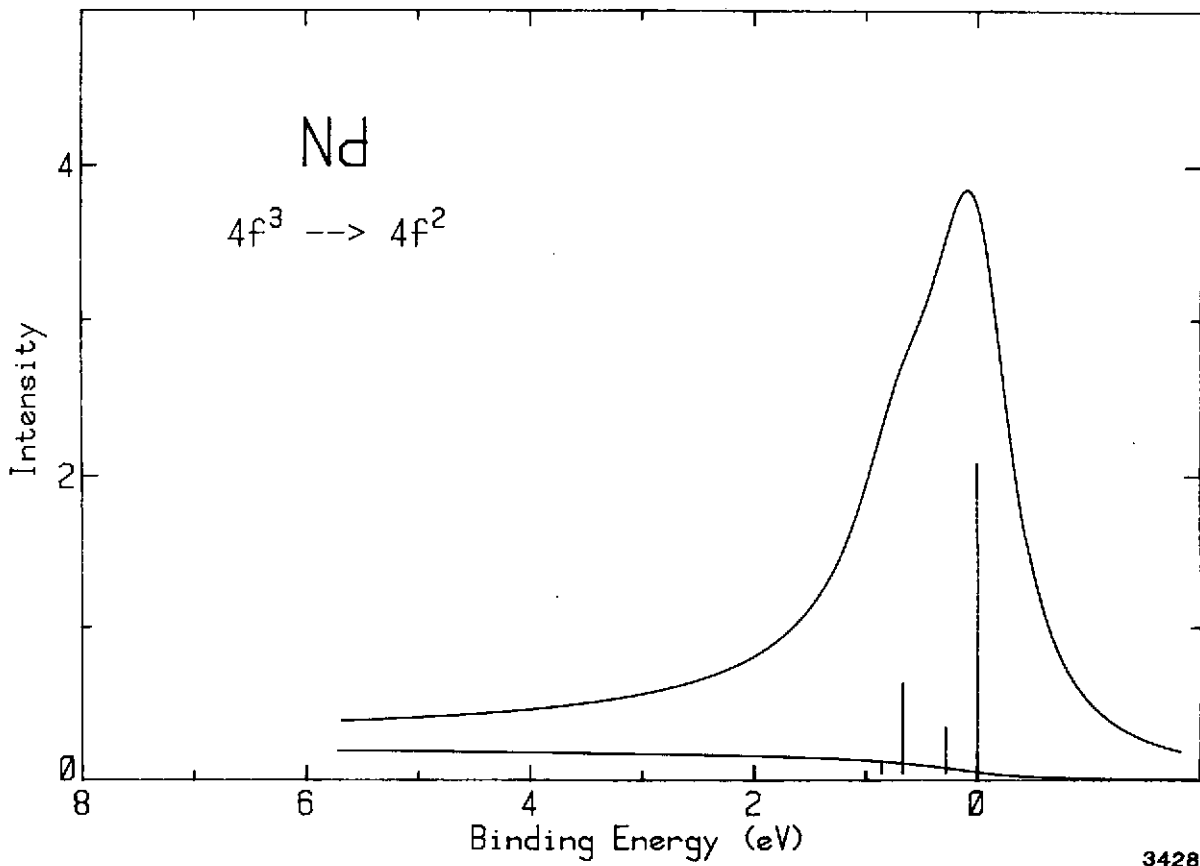


Fig. 1a

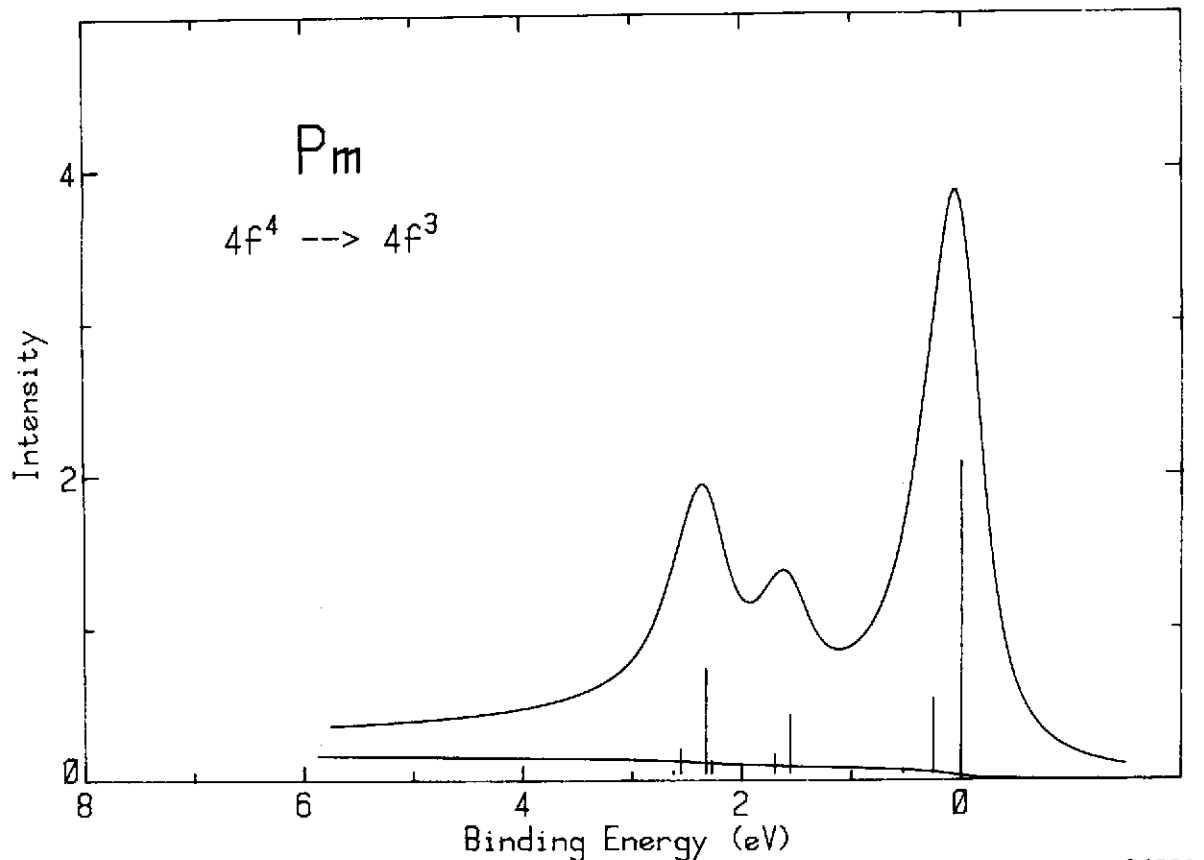


Fig. 1b

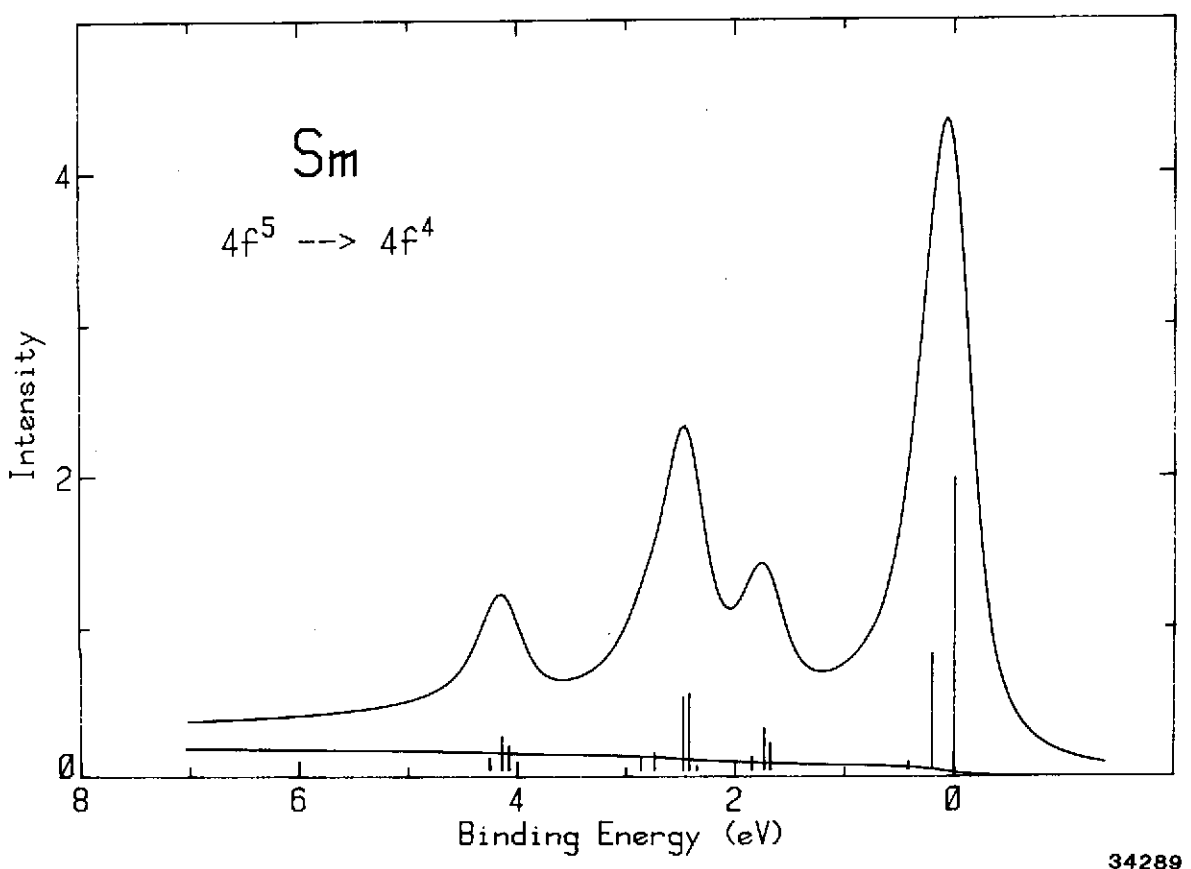


Fig. 1c

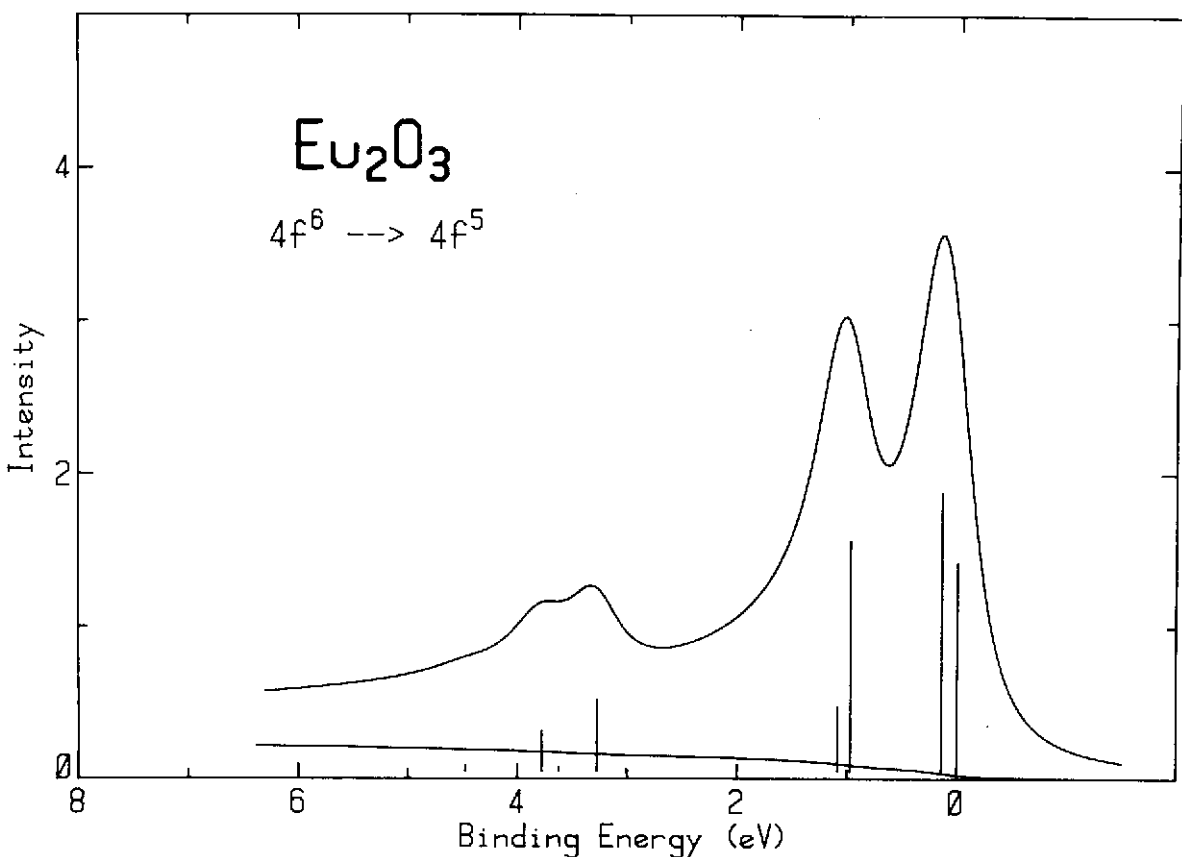


Fig. 1d

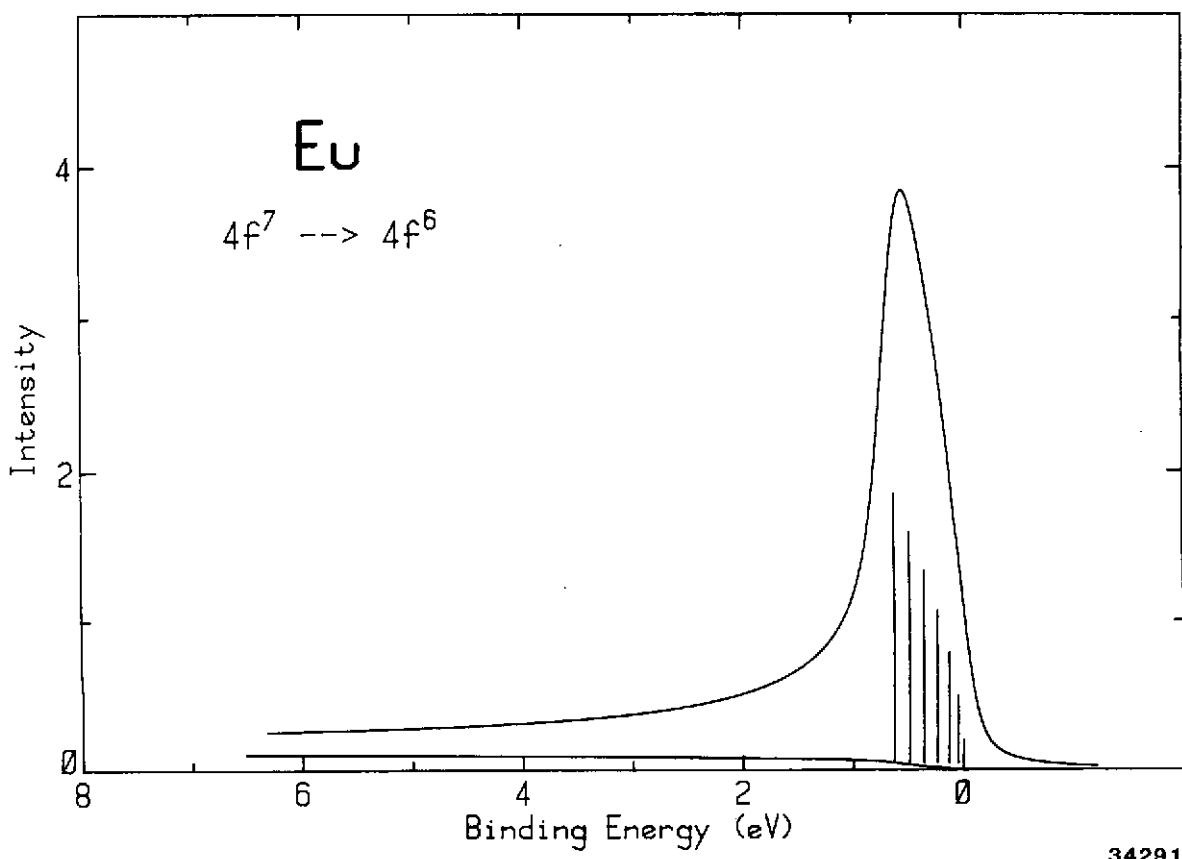


Fig. 1e

34291

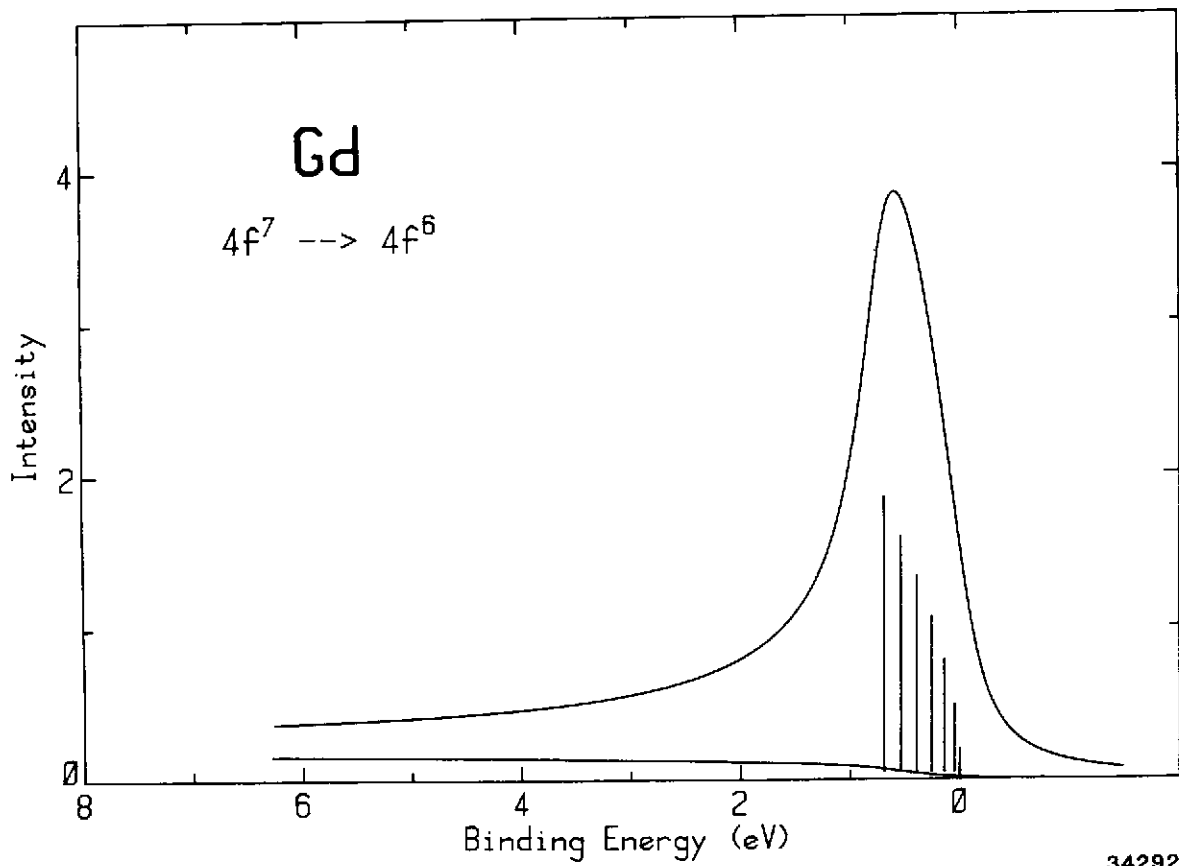


Fig. 1f

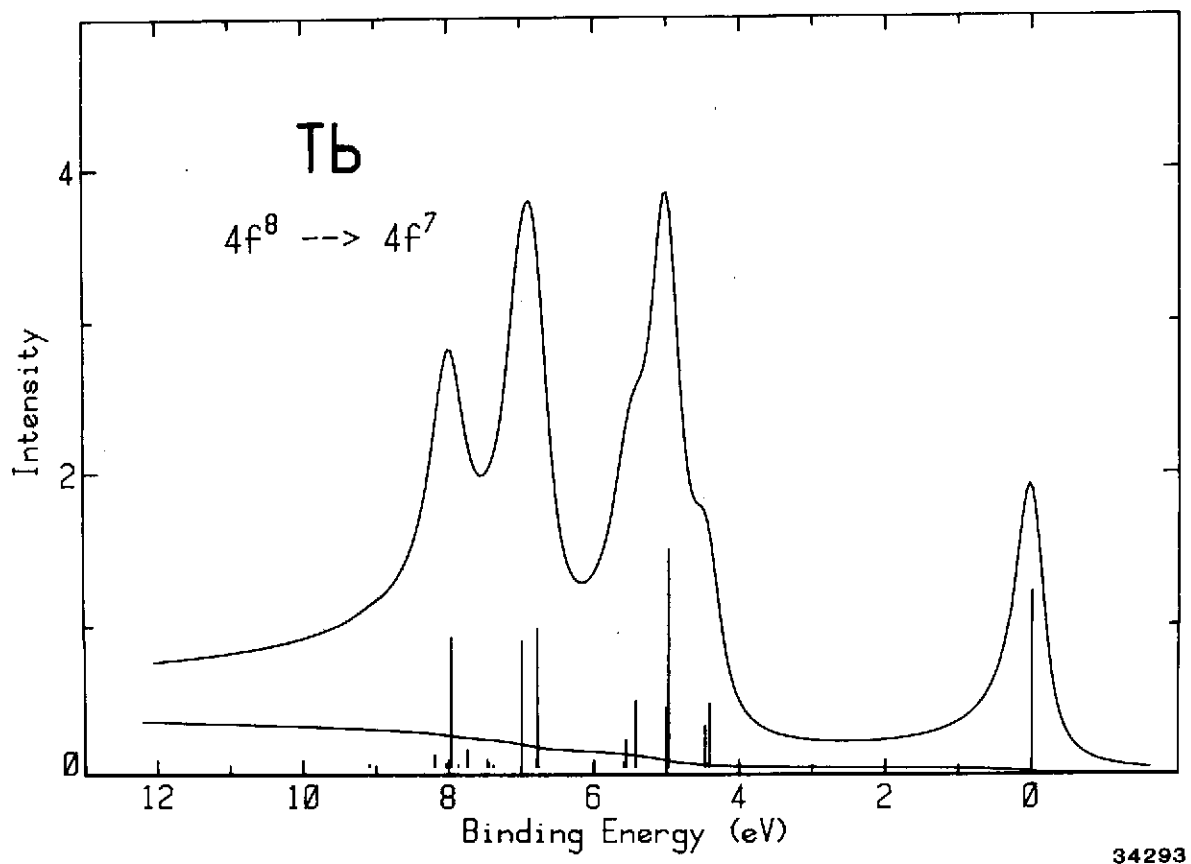


Fig. 1g

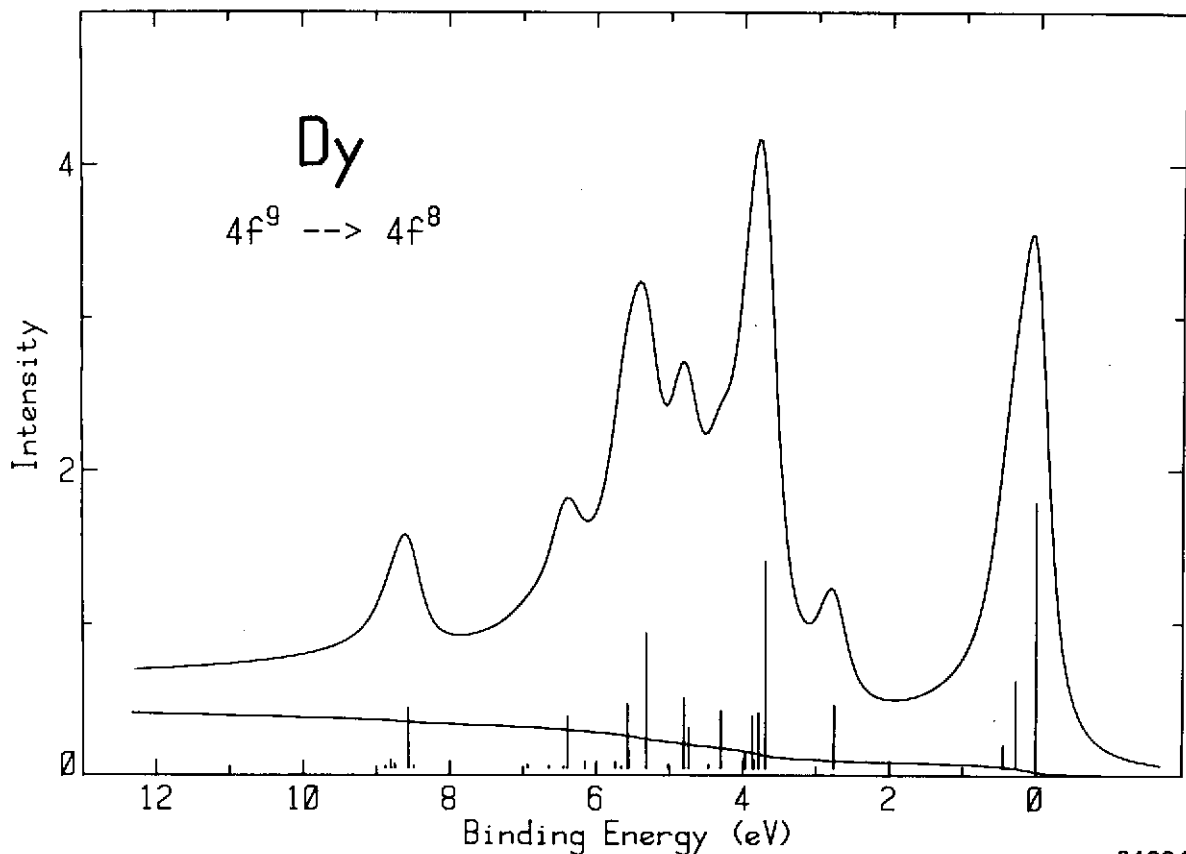


Fig. 1h

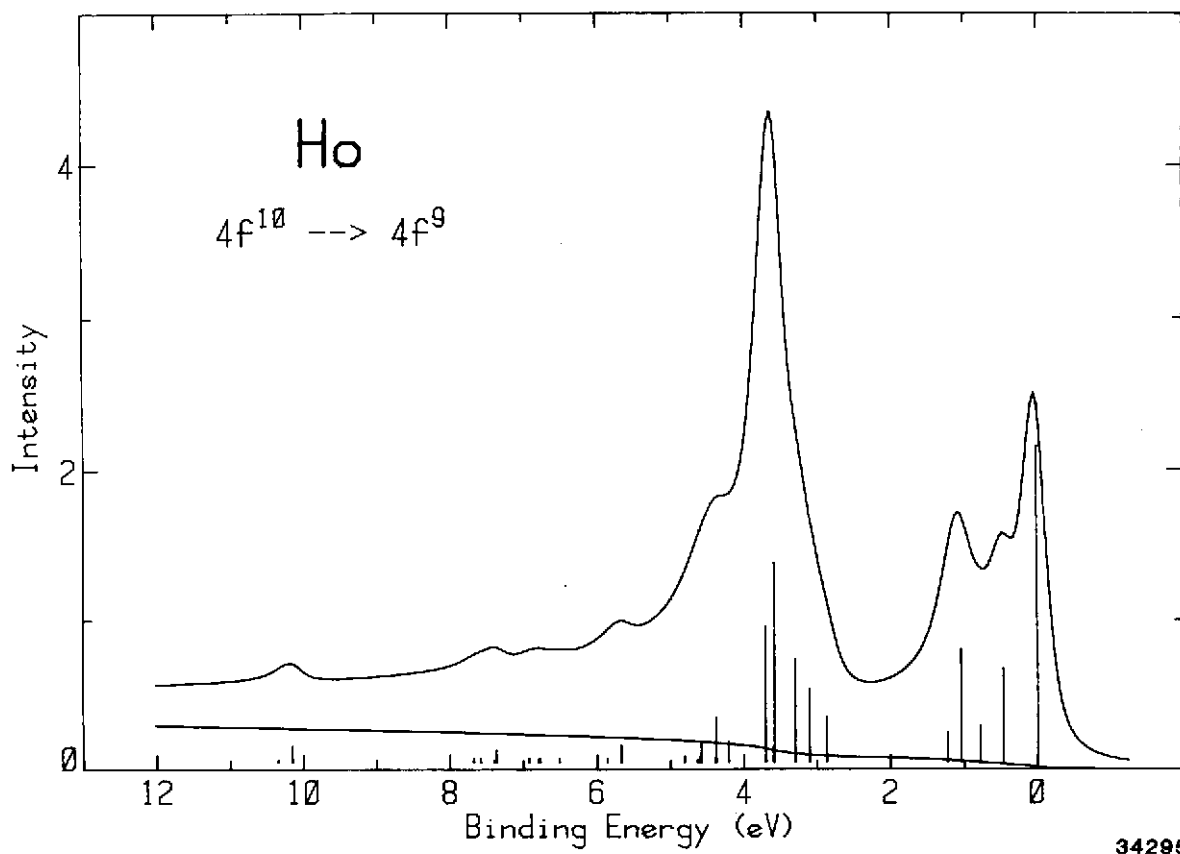
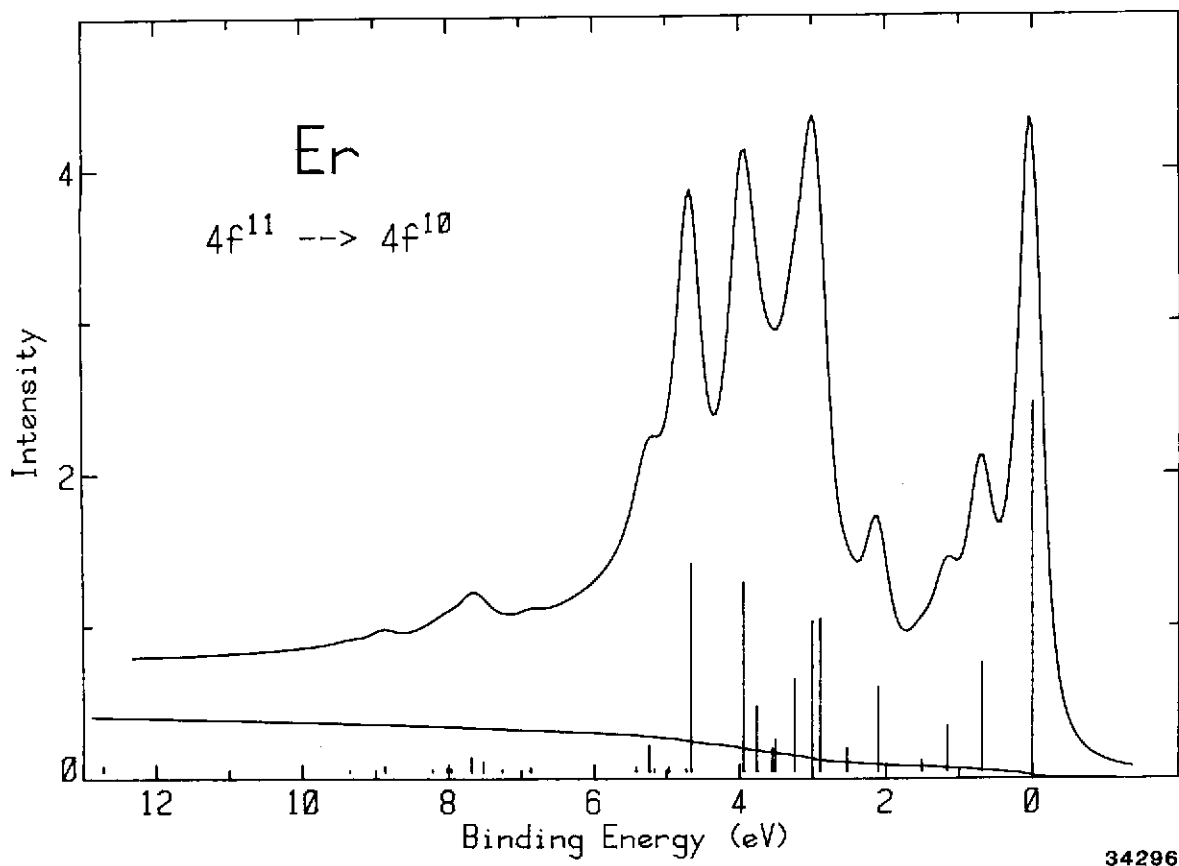
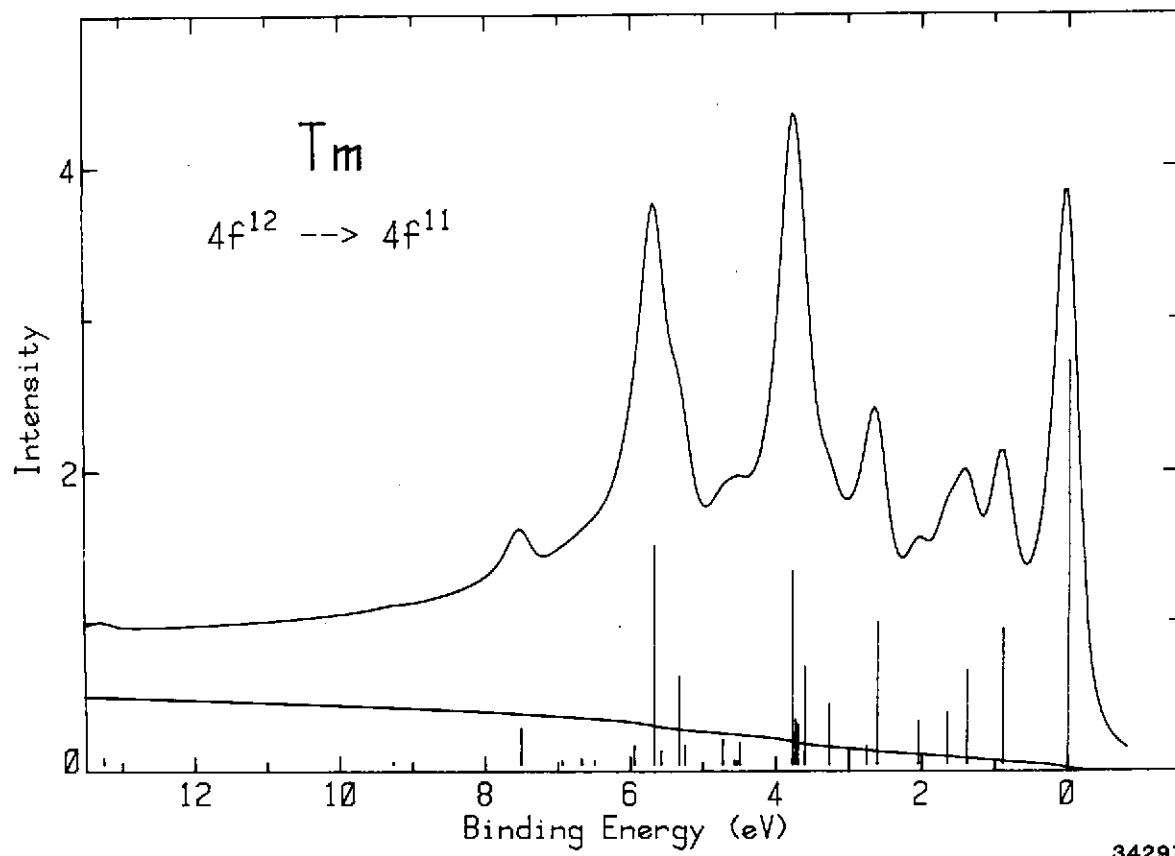


Fig. 11



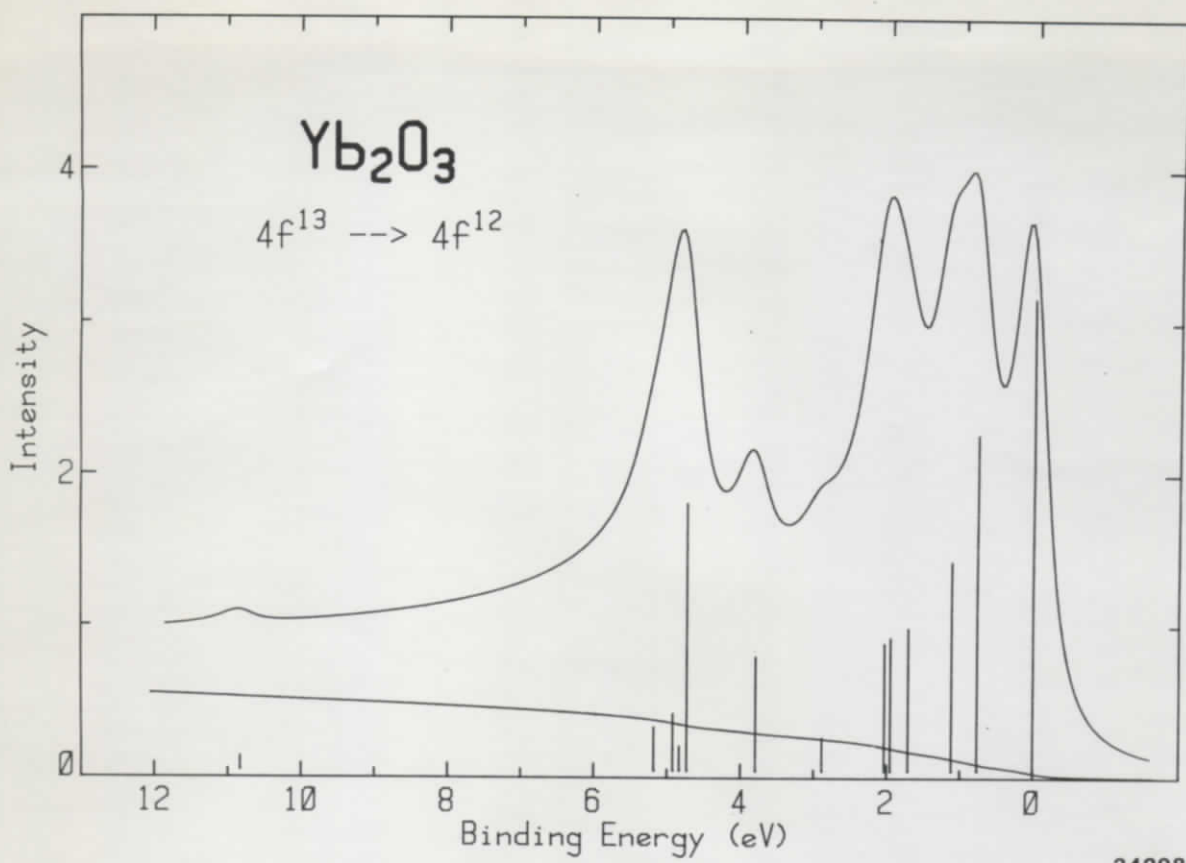
34296

Fig. 1k



34297

Fig. 11



34298

Fig. 1m

